

An Optimization Algorithm of Synthesizing a Feed-Forward Neural Network to Determine a Human Functional State Using Stabilometry Data

Ivan Stepanyan¹, Safa Hameed^{2*}

¹ *Mechanical Engineering Research Institute of the Russian Academy of Sciences (IMASHRAN) 4, M. Kharitonyevskiy Pereulok, 101990, Moscow, RUSSIAN FEDERATION*

² *Department of Mechanics and Control Processes, Academy of Engineering, Peoples' Friendship University of Russia named after Patrice Lumumba (RUDN University), Moscow, 117198, RUSSIAN FEDERATION*

*Corresponding Author: sa.programmer1@gmail.com
DOI: <https://doi.org/10.30880/jscdm.2025.06.03.006>

Article Info

Received: 26 May 2025
Accepted: 22 September 2025
Available online: 30 December 2025

Keywords

Feedforward neural network,
evolutionary algorithm,
optimization, crossover, mutation

Abstract

Balance is crucial to an individual's quality of life and functional performance. Stability measurement analysis and balance assessment rely on center-of-pressure coordinates and numerical data. Although machine learning algorithms have been applied to analyze stabilization measurements, accurately determining an individual's balance stability remains a challenge despite promising results. This study assesses the efficacy of a classification model—specifically, artificial neural networks (ANNs) utilizing an evolutionary algorithm (EA)—trained on three stability indicators to evaluate human health status. The methodology involved enhancing the learning process of artificial neural networks (ANNs) by dividing the hidden layers into multiple ANNs based on the number of neurons, optimizing them using an evolutionary algorithm, and then combining them to formulate new optimal hidden layers. This method expedited the optimization process and determined optimal designs. This study illustrates that optimal learning phases enhance the selection of appropriate artificial neural network architectures for distinguishing between healthy and diseased conditions, attaining accuracy rates of 99% to 100% for the A-indicator, 98% to 100% for the AW-indicator, and 97% to 100% for the AXI-indicator. The findings demonstrate that the integration of evolutionary algorithms and artificial neural networks markedly enhances predictive accuracy in healthcare, necessitating additional research to corroborate these results.

1. Introduction

Balance measurement is a diagnostic assessment used to test balance function and postural stability, both of which affect an individual's balance and quality of life. Functional balance assessment is critical for daily activities and is often performed using a computer-based platform for measuring installation thresholds and posture control. Balance problems greatly affect an individual's quality of life, especially in the elderly, as cognitive decline, language impairment and impaired decision-making ability increase the risk of falls. Over two-thirds of adults experience at least one fall annually [5–7], with balance disruption being the primary cause of these falls [8], [9]. To prevent balance disorders, early detection and management are critical, involving the identification of indicators such as ECG data, movement coordinate metrics, and body mass index. These parameters can be

This is an open access article under the CC BY-NC-SA 4.0 license.



integrated into intelligent systems to predict imbalances. Therefore, employing a precise tool that utilizes stability measurements to evaluate an individual's condition is essential.

Current machine learning algorithms can effectively map, classify, and rank factors influencing body sway. A recent survey of 209 studies demonstrated that machine learning techniques can distinguish healthy individuals with prediction accuracies ranging from 80% to 100% using various data sources. Static balance assessments show accuracies between 64% and 83.9%. Deep learning methods, such as artificial neural networks, employ multiple processing layers to learn data representations [9–17].

The research in this paper is based on stability measurement data defined by three indicators that reflect the dynamics of the tasks performed. The evaluation concentrated on the subject's overall center of pressure (OCP) placements on the support surface during the assessment, often characterized by several computed metrics [18]. The methodology employed a feedforward artificial neural network (FANN) combined with an evolutionary algorithm (EA) to evaluate human health based on these three factors. The evolutionary algorithm improves ANN learning process via altering the parameters through three basic steps, beginning with the breaking phase to accelerate the learning process. The artificial neural network is divided into layers based on the number of neurons, each requiring distinct optimization. The mutation stage uses an evolutionary algorithm to identify and optimize parameters for future generations through mutation and exchange. The final stage involves integrating the optimized artificial neural networks for each hidden layer to produce a new, improved artificial neural network. This integration produces optimized layers that enable the powerful artificial neural network to analyze data and predict human health conditions based on specific indicators. This integration improves model accuracy and facilitates adaptive learning, allowing artificial neural networks to continuously improve their predictions as new data emerges, enhancing their effectiveness in health analytics. Continuous refinement of artificial neural network models maintains their relevance in the face of rapid structural changes by adapting to new health trends, providing valuable insights, and improving patient outcomes through personalized healthcare solutions.

2. Literature Review

This paper analyzes diverse contributions to quantifying stability and evaluating human internal balance through artificial intelligence techniques. Despite the use of numerous effective models by researchers, these methods also present several challenges.

The study in [2] utilized gradient boosting models and artificial neural networks to distinguish between preserved and modified balance states. The study underscores the necessity of enhancing indications of balance behavior, since they can be assessed by stability measurement devices. A study in [3] analyzed force platform test results from 65 patients with balance impairments and 65 healthy individuals, finding that vertical posture regulatory patterns can be differentiated between healthy and stroke patients using energy intensity analysis with a Kohonen neural network. The relative strength of the clusters ranged from 78.95% to 99.07%. Nevertheless, the probability that a cluster's contents correspond to the specified category depends on comparison with a priori known properties of the individuals' conditions. The study in [4] examined the correlation between eyes-open and eyes-closed static balance and functional tests in individuals over 65 years old. Statistical studies were conducted utilizing Jamovi software version 1.6.23, employing the Kolmogorov-Smirnov test and Pearson's correlation coefficient. The research established that the Short Physical Performance Battery (SPPB) demonstrated the strongest correlation with normative values. However, as the study was conducted on healthy older individuals, its relevance to older adults with various medical issues is uncertain. The study in [8] examined the impact of aging on balance in healthy women, highlighting the limitations of tests that are limited to patients with specific abilities. Forty-nine healthy adult women participated in static posturography using the Romberg test. Results indicated maximal instability in the right groin (RGC) and a significant increase in anteroposterior oscillations associated with the left lumbar spine (ML), with no correlation to age. Although the study suggested that age may not influence the manifestation of balance abnormalities in the sampled women, several factors—such as muscle function characteristics—could independently affect balance loss. The study in [9] conducted supervised classification experiments on posturographic sway features from patients with vertigo, balance, and movement disorders. Quantitative static posturography proved useful for computer-aided diagnosis in certain cases. However, other stance disorders require more meaningful features, varied stance conditions, and multi-modal examinations. Mapping high-dimensional clinical data into a two-dimensional space can provide informative visualization. A limitation of the study is the significant age disparity between the healthy control (HC) group and seven illness groups, which may affect the classification accuracy of healthy controls due to aging effects. The study in [10] is about Parkinson's disease (PD). Postural instability leads to lower quality of life, as a study used a convolutional neural network to differentiate healthy individuals from those with early to mid-stage Parkinson's disease by analyzing spectral body vibrations. Despite the promising results recorded in [10], numerous limitations remain. The CNN results may not be applicable to other Parkinson's patient groups due to differences in age, disease duration, and medication dose between the Parkinson's patient group and the general

population. Furthermore, the results, based on a small and diverse sample, are preliminary and require validation on a larger and more diverse scale.

The study suggests three steps to enhance artificial neural networks using stability measurement data: splitting original FANN layers into multiple networks, using an evolutionary approach, and combining them to create a more robust FANN. This model can handle large datasets, assess age group health, and accurately predict outcomes without prior information.

3. Methodology

The proposed model includes a Functional Artificial Neural Network (FANN) together with an Evolutionary Algorithm (EA). The EA method was used to enhance the FANN learning process through three principal steps: first, breaking down the ANN layers into several smaller ANNs according to the neuron count in each layer to optimize each neuron independently; second, carrying out the EA algorithm; and finally, performing the combination process. The model utilized three stabilometry data indicators to predict human health status. The dataset comprises three time series indicators: A, AW, and AXY that represent work dynamics. The stabilometric dataset reflects the human condition, encompassing both health and disease states. It includes three time series datasets: A, AW, and AXY, each illustrating work dynamics. Indicator A contains 358 samples representing health and disease status, with 4,750 features each. The Indicator AW comprises 406 samples of health and disease status, also with 4,750 features. Indicator AXY includes 356 samples of health and disease status, encompassing 9,500 parameters, as detailed in Table 1. For each parameter, the stabilometric data is provided as a series of values. The specialists choose 19-second intervals to capture the data, with the frequency of 250 Hz. method has made the process of obtaining many ways easier. Data categorization happens locally within each track throughout durations corresponding to the recording duration, enabling the recognition and classification of localized features within a two-dimensional data array [19].

A study was conducted to analyze data from repeated assessments on a force platform in patients and healthy volunteers during the recovery phase following cerebral ischemic stroke. Participants followed a standardized protocol involving 30 seconds of quiet, upright bipedal standing on an ST-150 force platform. The results were evaluated using a method that assesses the energy efficiency of postural control in relation to interaction with the support surface. The key parameter in this approach is the energy intensity of the movement trajectory, expressed by the statokinesiogram (SKG) of the typical center of pressure. The study complied with established ethical standards, as outlined in Equation (1).

Table 1 *The indicators*

Indicator	Relevance	Number of parameters
A	Dynamics of work performed $A(i)=Ax(i)+Ay(i)$	4750
AXY	Dynamics of work in the X, Y coordinates	9500
AW	Dynamics of work in Z (weight)	4750

$$A = \sum_1^n A_i = m \sum_1^n \frac{|Vx_{i+1}^2 - Vx_i^2| + |Vy_{i+1}^2 - Vy_i^2|}{2} \quad (1)$$

In this context, x and y represent the coordinates of the patient's OCP within the stabilization platform coordinate system; m represents the patient's body weight; and Vxi and Vyi reflect the instantaneous velocities of the OCP. The SKG energy intensity calculated within a single estimation period Ai is called the "instantaneous energy intensity of the regulation", while the time sequence of its values Ai(t), similar to the stability diagrams Xi(t) and Yi(t), is referred to as the "energy stability diagram" (ESG) [20].

The research used Python as a programming platform due to its efficiency and ease of use in modeling. This strategy standardizes data processing and analysis, enabling scientists to quickly find results. Python's flexibility makes it easy to integrate multiple libraries, improving the overall performance of the system. The normalization tool enhances work classifier performance by preprocessing the dataset and applying "minimum and maximum feature measures" technique to the interval [0, 1]. This method uses the minimum and maximum values to normalize the data. Formally, it scales a vector x to the interval [0, 1], as shown in Equation (2) [21–23].

$$x_i = (x_{max} - x_{min}) * \frac{x_i - x_{min}}{x_{max} - x_{min}} + x_{min} \tag{2}$$

A proposed neuro-evolutionary phenotypic model consists of a multi-layer feedforward artificial neural network (FANN) and an evolutionary algorithm (EA). The FANN structure has input layer, four hidden layers, each with three neurons, and output layer. The ANN architecture undergoes optimization in phases, as illustrated in Fig. 1, which depicts the optimization process cycle. The optimization continues until the results meet or exceed a predefined threshold value. The process involves the following steps: (a) breaking down the FANN layers into multiple ANNs based on the number of neurons in the hidden layers; (b) mutating each ANN; (c) performing crossover within the synapses of the artificial neural networks; and (d) combining the optimized ANNs into an innovative, robust hidden layer. The phases continue until the desired objectives are accomplished. The iterative method of testing data after achieving goals enhances the efficiency and creativity of the model.

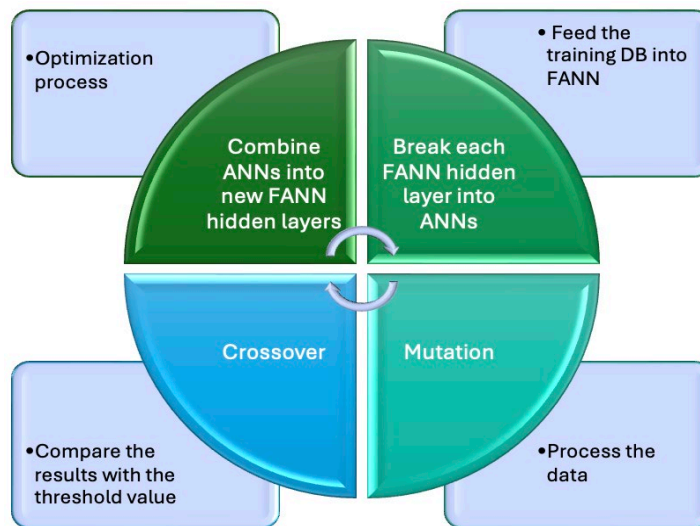


Fig. 1 The visual representation of the optimization process cycle

The range of data features is used to create a weight matrix, which is then multiplied by the input added with the bias as in Equation (3). The neurons in the hidden layer process the receiving data by using a ReLU function as in Equations (3) and (4); the output layer produces the outputs by using a ReLU function as in Equation (5); the output is compared with the threshold value, which is 0.5; the health status represents 1 if the values are greater than or equal to 0.5, while the illness status represents 0 if the values are less than 0.5, as in Equation (6), to do the classification. The outcome is next assessed versus a threshold of 0.5: a value of 1 indicates a healthy condition if it is bigger than or equal to 0.5, while a value of 0 indicates a diseased status if it is less than 0.5, as demonstrated in Equation (7) for classification goals [22-26]. The outcomes should prove inadequate; a learning process becomes important. The result is then compared to a threshold of 0.5: healthy status is indicated by 1 if values are greater than or equal to 0.5, while pathological status is indicated by 0 if values are less than 0.5, as shown in Equation (7) for classification purposes [22-26]. If the results are insufficient, a learning process becomes necessary.

$$s = \left(\sum_{i=1}^f W_i \cdot X_i \right) + b \tag{3}$$

$$\sigma = \max(0, s) \tag{4}$$

$$\text{neuron} = \sigma(s) = \sigma\left(\sum_{i=1}^f W_i \cdot X_i\right) + b \quad (5)$$

$$\hat{z} = \max\left(\sum_{j=1}^n W_j \cdot \text{neuron}_j\right) + b, \quad 0) \quad (6)$$

$$f(x) = \begin{cases} 1, & x \geq 0.5 \\ 0, & x < 0.5 \end{cases} \quad (7)$$

Where i represents the index of feature for each sample of data, f represents the number of features, W represents the weight, X represents the features, b represents the bias, σ represents the activation function (ReLU), neuron represents the output from the neuron, \hat{z} represents the output from FANN, n represents the number of neurons and j represents the index of neuron in layer.

3.1 Optimization Process

The system's implementation comprises two phases: training and testing for each indication. Eighty percent of the data was allocated for training, while the remaining twenty percent was reserved for testing. During the training phase, the training data is divided into multiple batches, each containing the two conflicting classes. The system extracts feature and applies regularization across all data characteristics. As the model trains on each batch, it gains competence from the conflicting classes; with each additional batch, it acquires insights from the diverse attributes of the competing samples. Through multiple phases of optimization, the system continues to train on the batches of data that are given to it.

The learning process consists of multiple stages designed to enhance the efficiency of the FANN. With each layer broke into multiple ANNs based on the number of neurons it has. To get the most out of each artificial neural network, we need an evolutionary strategy that uses more than one mutation and exchange operation. These superior artificial neural networks are then combined to create a new, better-performing FANN layer. The optimization process continues until the results are good enough, resulting in a new, highly efficient FANN. The system verifies the results of each iteration of the ANN during the optimization process to ensure consistent improvements. Feedback from the output layer during training is essential to help make adjustments that improve model accuracy.

3.1.1 Breaking Process

The initial stage in the optimization process is to divide the FANN layers into several artificial neural networks, one for each layer, based on how many neurons are in each layer. While one artificial neural network gets an appropriate solution the other artificial neural networks begin to improve it. This incrementally method enhances the learning process by permitting each artificial neural network work on its own while distributing what it finds out as it passes along. This allows the artificial neural network (FANN) operate much better, which means it becomes to a solution more quickly and precisely. The ANNs created in the input layer require an effective optimization technique to produce acceptable outputs. Equation (8) indicates that the list retains the optimal artificial neural networks from the current hidden layer. This process continues until all neurons in the current hidden layer are optimized. The optimization procedure for each neuron is repeated for every hidden layer, as illustrated in Fig. 2(a).

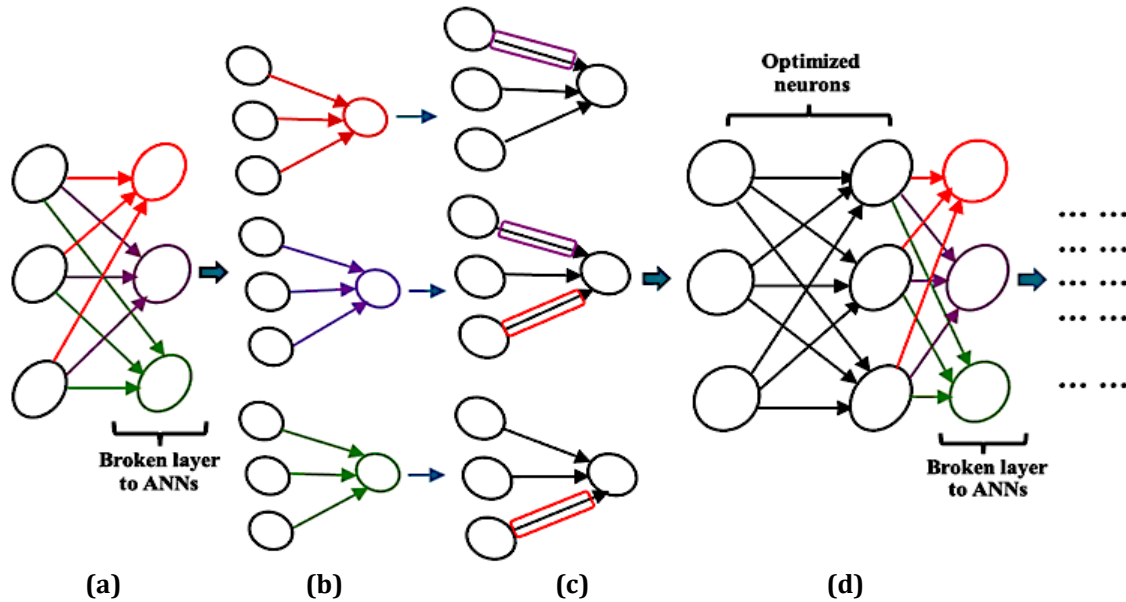


Fig. 2 The optimization stages: (a) breaking; (b) mutation; (c) crossover; and (d) combination

3.1.2 The Mutation

The mutation method partitions artificial neural networks (ANNs) by threshold condition to simplify optimal outcome evaluation. Each ANN undergoes random mutations, and the modified structure is evaluated against the threshold to assess network performance. The adjusted ANNs are then stored in the list as specified in Equation (8).

This process, which is performed repeatedly, improves the efficiency of the network and maintains optimal settings for subsequent training. It also improves the efficiency of the entire system, allowing it to produce better predictions and perform better with diverse datasets. Mutation has improved the artificial neural network, as shown in Fig.2(b). This strategy ensures that each iteration is better than the previous one, resulting in an efficient framework that can handle difficult problems. Adding feedback also facilitates rapid changes, helping individuals learn and achieve optimal results. The pseudocode and the flowchart in Fig. 3 clarify the way to generate artificial neural networks.

$$ANNs = [[ANN_{i_1}, \dots, ANN_{n_1}], \dots [ANN_{i_j}, \dots, ANN_{n_j}]] \tag{8}$$

Where, i represents the index of neuron, j represents the index of layer, n represents number of neurons in the layer and L represents number of layers.

Pseudo code:

```

1: C ← 0
2: Batch ← 0
3: Btch ← batches
4: Loop (i, layers):
5:   While (False):
6:     Loop (j, neurons):
7:       While (False):
8:         Loop (k1, batches):
9:           Loop (k2, samples):
10:            sop ← sum_of_product (weight, x) + bais
11:            r ← Relu (sop)
12:            If Target >= threshold:
13:              If r >= threshold:
14:                C ← C + 1
15:              Else:
16:                If r < threshold:
17:                  C ← C + 1
18:            If C == samples:
19:              Batch ← Batch + 1
20:            If Batch == Btch:
21:              new_weight ← weight
22:            Else:
23:              weight ← mutation(weight)
24:          If j == neurons:
25:            new_weight [j] ← w
26:            new_weight [j] ← new_weight [j-1]
27:            new_weight [j-1] ← w
28:          check (new_weight, x)

```

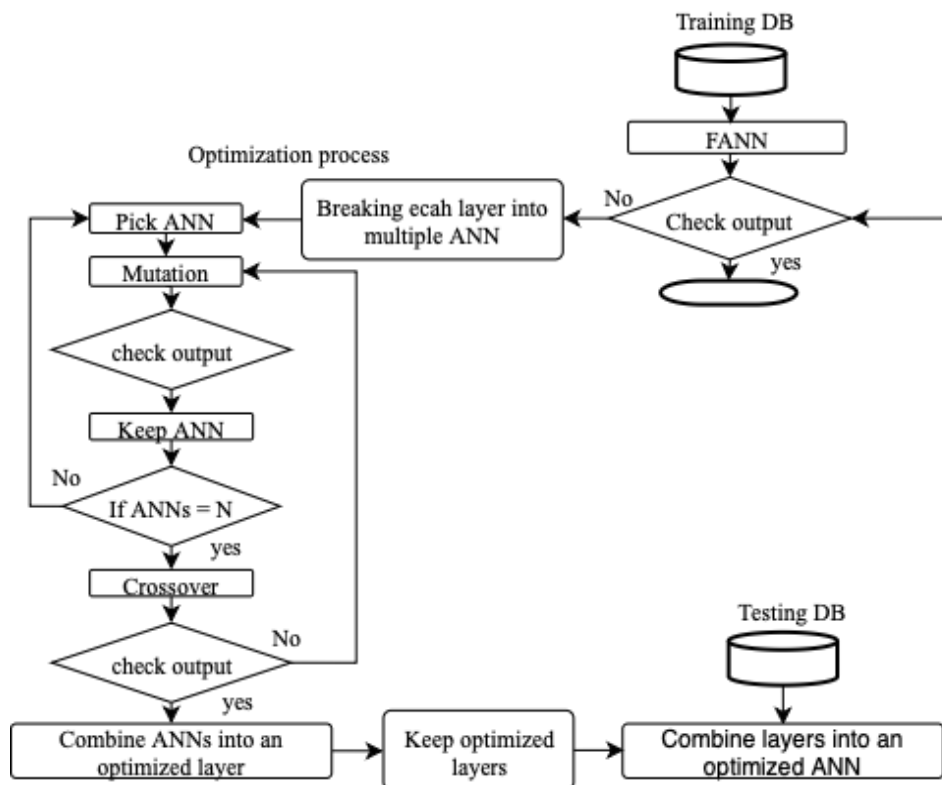


Fig. 3 The flowchart of neuro evolutionary model

3.1.3 The Crossover

The crossover method employs artificial neural networks (ANNs) that were created for the current layer after the mutation phase. After developing ANNs for each neuron in the present layer, the crossover operates on the premise that the ANNs correspond to the number of neurons in that layer. The designated parameters of the ANNs are enhanced by interchanging the synapses of neurons while maintaining the same index, as demonstrated in equation (8). The crossover process simplifies learning and transfer processes in artificial neural networks, enhancing their effectiveness in accurately predicting and identifying complex patterns in datasets as in Fig. 2(c).

$$F(ANN_{ij}, ANN_{i-1j}) = F(ANN_{k_{ij}}, ANN_{k_{i-1j}}) = ANN_{k_{ij}} \Leftrightarrow ANN_{k_{i-1j}} \quad (8)$$

Where i represents index of neuron, j represents index of layer and k represents index of synaptic.

3.1.4 Combining Process

The system undergoes regular modifications and improvements to ensure it meets performance standards before the final evaluation. Tuning allows for necessary adjustments, resulting in a more robust neural network. Fig. 2(d) illustrates how neural networks with improved neurons are combined to create a new best hidden layer, with a threshold value used to determine if the output is satisfactory, and the method continues to optimize the next layer. The hidden layer will be refined sequentially to enhance the overall framework's performance by modifying each layer accordingly. Thus, the neural network becomes more accurate while minimizing the use of computing resources, resulting in higher accuracy in its results. The optimization step is critical for challenging tasks, because even small adjustments can significantly impact how well the network utilizes the data used for training. Therefore, it is necessary to continuously evaluate and develop AI systems to make them more powerful

4. Results and Discussion

The method was employed to assess human health and illness cases by utilizing stability data from three different factors. The system's implementation consists of two stages: training and testing for each indication. Eighty percent of the data was allocated for training, while the remaining twenty percent was designated for testing. The division ensures thorough testing of the model's performance to prevent overfitting. Researchers aim to enhance the method's accuracy in predicting health consequences by analyzing data from the testing phase, providing a comprehensive evaluation of the model's performance and reducing overfitting. The methodology was modified based on test results analysis to enhance its accuracy in predicting health outcomes, with training data divided into multiple batches with two different classes. The system extracts features from these classes and applies regularization to all data features. While training on a single batch, the model assimilates information from the competing classes; upon processing additional batches, it gains insights from the diverse characteristics of the conflicting samples. The system continuously trains on the supplied data batches through multiple iterations, as shown in Tables 1, 3, and 5, until the criteria for improved accuracy are met. Each set of indicators contains examples of both healthy and sick individuals. The dataset is divided into two subsets, with 80% of it being utilized for model training.

The FANN training process involves four layers with three neurons each, and the learning process divides the network into three artificial neural networks (ANNs) for each layer. The ANNs check each neuron against a 0.5 threshold value to determine if the person is healthy or sick. The optimized ANN is derived from the initially flawed feedforward artificial neural network (FANN), which has undergone multiple rounds of crossover and mutation. The ANN continues to learn until it surpasses a predefined threshold value. Upon completion of this process, additional neurons apply the same method to represent the optimized networks derived from the compromised original FANN. Following the target for training has been achieved, the system undergoes evaluation by entering test data to determine how precise the testing matches up to the training phase. The optimized ANNs are then combined to form a robust FANN, and the training data is input into this newly merged FANN to assess training accuracy.

Table 2 describes the model optimization phase for indicator A. During the training phase, the original FANN is divided into multiple ANNs, each optimizing a specific neuron. Each neuron is then enhanced through a mutation process involving numerous iterations. The crossover operation is performed by exchanging the synapses of the optimized neurons. After a set number of learning iterations for each optimized ANN, the accuracy of each sample is evaluated to determine whether it meets the threshold condition. The accuracy of each state is assessed and represented by the variables H and I , which correspond to health and illness cases, respectively. The training and testing phases are thoroughly explained in Table 3. The values of H and I represent the final accuracy obtained from the last iteration of the training phase.

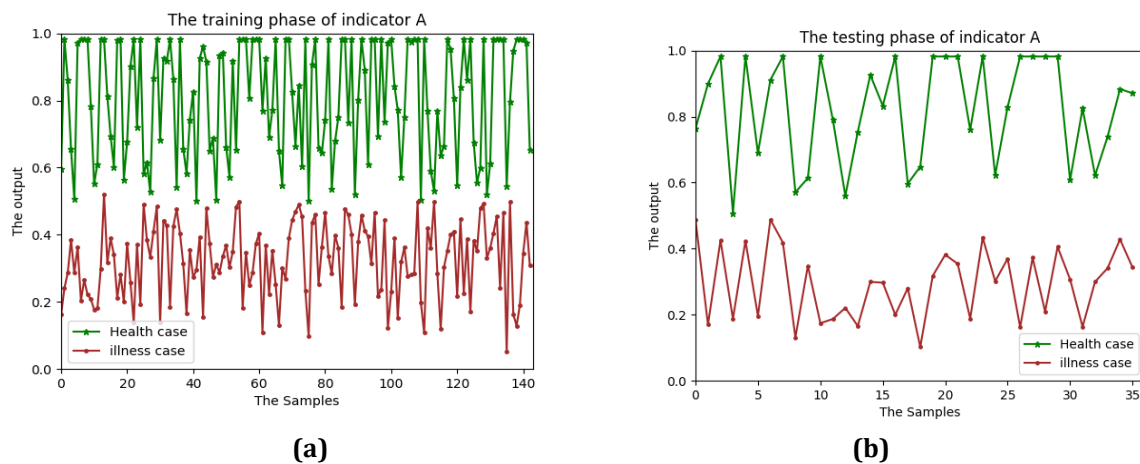
Table 2 The model optimization phase of the indicator A

ANNs	AH	I	Iterations	ANNs	H	I	Iterations
ANN_{1_1}	100.0	98.601	18630	ANN_{3_1}	100.0	96.503	81
ANN_{1_2}	100.0	99.3	55991	ANN_{3_2}	100.0	94.406	219
ANN_{1_3}	100.0	95.804	53733	ANN_{3_3}	100.0	96.50	228
ANN_{2_1}	100.0	99.3	412	ANN_{4_1}	100.0	96.503	84
ANN_{2_2}	100.0	94.406	438	ANN_{4_2}	100.0	96.503	156
ANN_{2_3}	100.0	94.406	536	ANN_{4_3}	100.0	96.503	89

Table 3 The training and testing phases accuracy of the indicator A

The phase	AH	I
The training phase	100.0	99.3
The testing phase	100.0	100.0

Fig. 4(a) shows the output for each sample in both the healthy and ill states of indicator A during the training phase. Samples representing a healthy status have condition values equal to or greater than the threshold of 0.5, while samples representing an ill status have condition values below this threshold. Fig. 4(b) presents the results for each sample in both healthy and ill states of indicator A during the testing phase.

**Fig. 4** The output of indicator A in (a) The training phase; (b) The testing phase

The indicator AW's model optimization phase is detailed in Table 4. The number of learning iterations for each optimized ANN is recorded, and the accuracy for each sample is evaluated to determine whether it meets the threshold criterion. The variables H and I, representing healthy and diseased cases respectively, are used to assess and illustrate the accuracy for each condition, as shown in Table 4. The values of H and I represent the accuracy achieved in the final iteration of the training phase, as well as the accuracy obtained during the testing phase.

Table 4 The training and testing phases accuracy of the indicator AW

ANNs	awH	I	Iterations	ANNs	H	I	Iterations
ANN_{11}	100.0	98.148	1327	ANN_{31}	100.0	95.679	111
ANN_{12}	100.0	96.296	286	ANN_{32}	100.0	95.679	163
ANN_{13}	100.0	96.914	2452	ANN_{33}	100.0	97.531	120
ANN_{21}	100.0	97.53	1235	ANN_{41}	100.0	98.765	152
ANN_{22}	100.0	98.765	1221	ANN_{42}	100.0	96.296	356
ANN_{23}	100.0	98.765	849	ANN_{43}	100.0	96.91	384

Table 5 The model optimization phase of the indicator AW

The phase	awH	I
The training phase	100.0	98.148
The testing phase	100.0	100.0

Fig. 5(a) shows the output for each sample of indicator AW in both healthy and diseased states throughout the training phase. The condition values for the diseased samples are below the threshold of 0.5, while those for the healthy samples are equal to or above this threshold. Fig. 5(b) presents the results for each sample of indicator AW in both healthy and diseased states during the test phase.

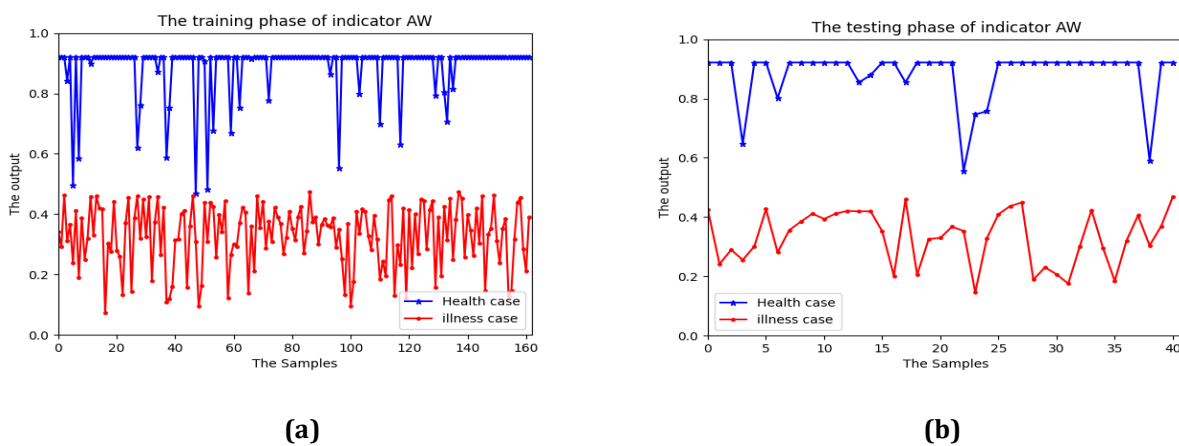


Fig 5 The output of indicator AW in (a) The training phase; (b) The testing phase

Table 6 outlines the model optimization phase for the indicator AXY. To determine whether an optimized artificial neural network (ANN) meets the threshold criteria, we count the number of learning iterations for each ANN and analyze the accuracy for each sample. As shown in Table 7, the correctness of each condition is evaluated and represented by the variables H and I, which correspond to the health and disease cases, respectively, during both the training and testing phases. The values of H and I indicate the accuracy achieved in the final iteration of the training phase.

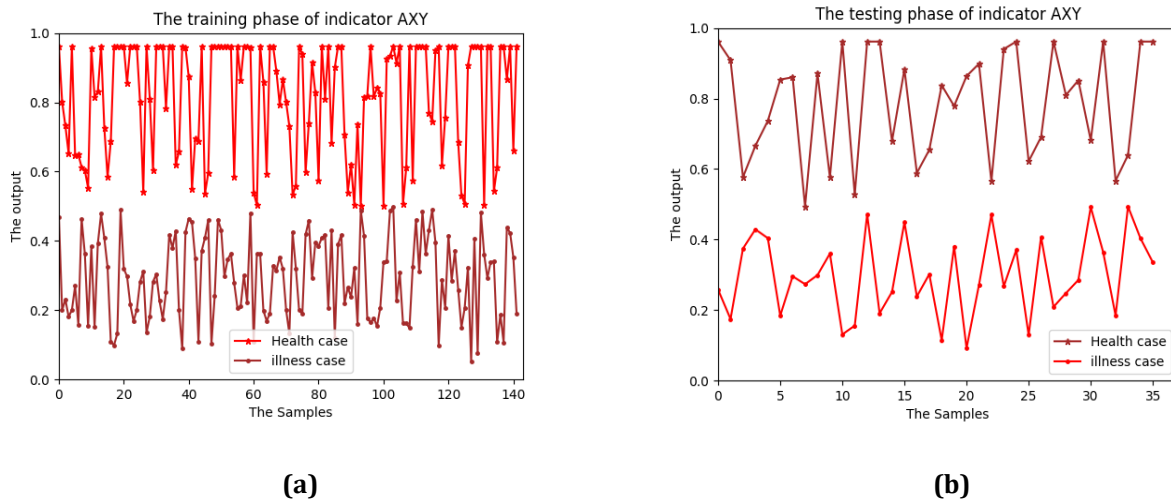
Table 6 The model optimization phase of the indicator *AXY*

ANNs	axyH	I	Iterations	ANNs	H	I	Iterations
ANN_{1_1}	99.296	95.105	7368	ANN_{3_1}	100.0	96.503	375
ANN_{1_2}	100.0	96.503	16486	ANN_{3_2}	100.0	97.902	488
ANN_{1_3}	100.0	98.601	16810	ANN_{3_3}	100.0	97.902	246
ANN_{2_1}	100.0	95.105	2634	ANN_{4_1}	100.0	94.406	386
ANN_{2_2}	100.0	94.406	2559	ANN_{4_2}	100.0	96.503	70
ANN_{2_3}	100.0	94.406	2798	ANN_{4_3}	100.0	95.105	430

Table 7 The training and testing phases accuracy of the indicator *AXY*

The phase	axyH	I
The training phase	100.0	100.0
The testing phase	100.0	97.222

Fig. 6(a) shows the output for each sample of indicator *AXY* during the training period, distinguishing between healthy and sick instances. The condition values for healthy samples are equal to or greater than the threshold value of 0.5, while those for sick samples fall below this threshold. Fig. 6(b) displays the results of each *AXY* index sample during the testing phase, separating healthy and diseased conditions.

**Fig. 6** The output of indicator *AXY* in (a) The training phase; (b) The testing phase

The objective of this research was to assess health status using a stabilometric dataset based on three indicators. The proposed model achieved excellent accuracy across all three indicators, resulting in a robust FANN structure derived from the optimization process that can effectively predict human health status. The breaking process facilitates optimization by evaluating each neuron independently, while the mutation stage in the evolutionary algorithm plays a significant role in enhancing neurons during this phase. The model optimization enhances learning experience by supporting numerous features and generalizing to diverse samples. It achieves over 99% accuracy in training and testing phases for all three indicators. The model's potential for practical use is evident under controlled conditions, as it optimizes neural networks, improving learning capacity and accuracy. Future research should focus on improving batching processes and adding more features. Comparing the model to stabilometry data methods, Table 7 shows it is more accurate and useful, making it a strong contender for real-world use. Future research may explore improving the batching process and adding more features. Subsequent studies will aim to optimize the algorithms and examine additional variables that could further improve predictive efficiency.

Table 8 *The comparison of the related approaches with the proposed model*

The Source, year	The dataset	The model	The evaluation
[2], 2023	Santos and Duarte dataset	XGBoost and artificial neural network multilayer perceptron models	Testing Accuracy: 0.718; Recall: 0.722
[3], 2023	Stabilometric dataset [19]	Self-organizing Kohonen networks	78.95% - 99.07%
[4], 2022	Stabilometry data were collected using SPPB, 4WT, 5XSST, and TUG.	The Satel 40 Hz stabilometric force system.	High-performance correlation analysis
[9], 2019	Dataset of body sway metrics acquired using posturography sensor hardware	ANNMulti, RandForest, ExtraForest.	76.7% (kNN) to 93.3% (ANNMulti, RandForest, ExtraForest).
[10], 2025	idiopathic PD dataset collected	convolutional neural network	85%-100%
[15], 2022	Balance Control Data	Dempster–Sahfer formalism	96%
The proposed model, 2025	Stabilometric data set [19]	Neuro phenotype evolutionary model	99%-100%

5. Conclusion

The integrated approach combines an artificial neural network (ANN) algorithm with an evolutionary algorithm (EA). We tested the effectiveness of the system using the recommended approach on a stability assessment dataset containing three indices: A, AW, and AXY. The data were integrated into a multi-layer feed-forward artificial neural network (FANN). When comparing the acquired results for evaluation and verification between the two classes—health and illness—the threshold value is employed. To start the optimization process, each hidden layer is broken up into multiple ANNs based on the number of neurons. Every generation of the learning process for each ANN undergoes the crossover and mutation phases, which the evolutionary algorithm optimizes a new, effective FANN structure, the procedure is repeated for each hidden layer to be optimized. The system's implementation produced a high accuracy rate on a dataset in the training and testing stages. This accomplishment points out the importance of utilizing evolutionary algorithms in neural network design. As the model evolves, it may adapt to various data patterns, thereby enhancing its performance across multiple applications.

Acknowledgement

The work was carried out within the framework of the State assignment, the code of the scientific topic FFGU-2024-0019

Conflict of Interest

There is no interest between the co-authors.

Author Contribution

The authors confirm contribution to the paper as follows: **Study conception and design:** Safa H, Ivan S; **data collection:** Ivan S; **analysis and interpretation of results:** Safa H; **draft manuscript preparation:** Safa H. The authors reviewed the results and approved the final version of the manuscript.

References

- [1] Takada, H., Ono, R., Nakane, K., Kinoshita, F., & Nakayama, M. (2021) Stabilometry. *Bio-information for Hygiene*, 93-111. https://doi.org/10.1007/978-981-15-2160-7_9.
- [2] Montenegro, A., Sosa, G., Figueroa, N., Vargas, V., & Franco, H. (2023) Evaluation of stabilometry descriptors for human balance function classification using diagnostic and statokinesigram data. *Biomedical Signal Processing and Control*, 84, 104861. <https://doi.org/10.1016/j.bspc.2023.104861>.

- [3] Stepanyan, I. V., Grokhovskii, S. S., Yastrebtsseva, I. P., & Kubryak, O. V. (2023) Identification of physiological and pathological patterns of vertical posture regulation using a kohonen neural network with stabilometry data. *Biomedical Engineering*, 57(1), 61-64. <https://doi.org/10.1007/s10527-023-10268-w>.
- [4] Labata-Lezaun, N., González-Rueda, V., Rodríguez-Sanz, J., López-de-Celis, C., Llurda-Almuzara, L., Rodríguez-Rubio, P. R., & Pérez-Bellmunt, A. (2022) Correlation between physical performance and stabilometric parameters in older adults. *Medicina*, 58(9), 1211. <https://doi.org/10.3390/medicina58091211>.
- [5] Alfaya, F. F., Reddy, R. S., Alshahrani, M. S., Gautam, A. P., Mukherjee, D., Al Salim, Z. A., ... & Jabour, A. A. (2023) Exploring the interplay of muscular endurance, functional balance, and limits of stability: a comparative study in individuals with lumbar spondylosis using a computerized Stabilometric force platform. *Life*, 13(10), 2104. <https://doi.org/10.3390/life13102104>.
- [6] Rodríguez-Rubio, P. R., Bagur-Calafat, C., López-de-Celis, C., Bueno-Gracia, E., Cabanas-Valdés, R., Herrera-Pedroviño, E., & Girabent-Farrés, M. (2020) Validity and reliability of the satel 40 HZ stabilometric force platform for measuring quiet stance and dynamic standing balance in healthy subjects. *International Journal of Environmental Research and Public Health*, 17(21), 7733. <https://doi.org/10.3390/ijerph17217733>.
- [7] Quialheiro, A., Maestri, T., Zimmermann, T. A., da Silva Ziemann, R. M., Silvestre, M. V., Maio, J. M. B., ... & Martins, D. F. (2021) Stabilometric analysis as a cognitive function predictor in adults over the age of 50: A cross-sectional study conducted in a memory clinic. *Journal of Bodywork and Movement Therapies*, 27, 640-646. <https://doi.org/10.1016/j.jbmt.2021.04.007>.
- [8] Escamilla-Martínez, E., Gómez-Maldonado, A., Gómez-Martín, B., Castro-Méndez, A., Díaz-Mancha, J. A., & Fernández-Seguín, L. M. (2021) An assessment of balance through Posturography in healthy about women: an observational study. *Sensors*, 21(22), 7684. <https://doi.org/10.3390/s21227684>.
- [9] Ahmadi, S. A., Vivar, G., Frei, J., Nowoshilow, S., Bardins, S., Brandt, T., & Krafczyk, S. (2019) Towards computerized diagnosis of neurological stance disorders: data mining and machine learning of posturography and sway. *Journal of Neurology*, 266, 108-117. <https://doi.org/10.1007/s00415-019-09458-y>.
- [10] Engel, D., Greulich, R. S., Parola, A., Vinehout, K., Student, J., Waldthaler, J., ... & Bremmer, F. (2025) Sway frequencies may predict postural instability in Parkinson's disease: a novel convolutional neural network approach. *Journal of NeuroEngineering and Rehabilitation*, 22(1), 29. <https://doi.org/10.1186/s12984-025-01570-7>.
- [11] Hernandez-Laredo, E., Estévez-Pedraza, Á. G., Santiago-Fuentes, L. M., & Parra-Rodríguez, L. (2024) Optimizing Fall Risk Diagnosis in Older Adults Using a Bayesian Classifier and Simulated Annealing. *Bioengineering*, 11(9), 908. <https://doi.org/10.3390/bioengineering11090908>
- [12] Sihag, G., Delcroix, V., Grislin-Le Strugeon, E., Siebert, X., Piechowiak, S., Gaxatte, C., & Puisieux, F. (2021) Evaluation of risk factors for fall in elderly using Bayesian networks: A case study. *Computer Methods and Programs in Biomedicine Update*, 1, 100035. <https://doi.org/10.1016/j.cmpbup.2021.100035>.
- [13] Istomina, T., Istomin, V., Lafitskova, M., Nikitina, A., & Mozhakova, O. (2020, March) Fuzzy Classification of Romberg Test Parameters Using Verified Database of Stabil-Metric Data. *In 2020 International Youth Conference on Radio Electronics, Electrical and Power Engineering (REEPE)*, 1-4. IEEE., doi: 10.1109/REEPE49198.2020.9059166.
- [14] Castro, F., Savaris, W., Araujo, R., Costa, A., Sanches, M., & De Carvalho, A. (2020) Plantar pressure measurement system with improved isolated drive feedback circuit and ANN: Development and characterization. *IEEE Sensors Journal*, 20(19), 11034-11043. DOI: 10.1109/JSEN.2020.2998700.
- [15] Safi, K., Aly, W. H. F., AlAkkoumi, M., Kanj, H., Ghedira, M., & Hutin, E. (2022) EMD-based method for supervised classification of Parkinson's disease patients using balance control data. *Bioengineering*, 9(7), 283. <https://doi.org/10.3390/bioengineering9070283>.
- [16] Azevedo, N., Ribeiro, J. C., & Machado, L. (2022) Balance and posture in children and adolescents: A cross-sectional study. *Sensors*, 22(13), 4973. <https://doi.org/10.3390/s22134973>.
- [17] Andrii, C., Marina, K., Ruslan, A., Ivan, S., & Andrii, H. (2020) The Impact of Training Load on the State of the Vestibular System of Athletes specializing in Hand-to-Hand Combat. *Journal of Physical Education and Sport*, 20(3), 1628-1636. DOI:10.7752/jpes.2020.03222.
- [18] Duarte, M. & Zatsiorsky, V. M. (1999) Patterns of center of pressure migration during prolonged unconstrained standing. *Motor Control*, 3(1), 12-27.

- [19] MERA Research Center; 141002, Russia, Moscow region.
- [20] Grokhovskii, S. S. & Kubryak, O. V. (2018) A method for integral assessment of the effectiveness of human posture regulation. *Meditinsk. Tekhn.*, (2), 49–52.
- [21] Singh, D., & Singh, B. (2020) Investigating the impact of data normalization on classification performance. *Applied Soft Computing*, 97, 105524. doi: <https://doi.org/10.1016/j.asoc.2019.105524>.
- [22] Singh, D., & Singh, B. (2022) Feature wise normalization: An effective way of normalizing data. *Pattern Recognition*, 122, 108307. <https://doi.org/10.1016/j.patcog.2021.108307>.
- [23] Chanal, D., Steiner, N. Y., Chamagne, D., & Pera, M. C. (2021, October) Impact of standardization applied to the diagnosis of LT-PEMFC by Fuzzy C-Means clustering. In *2021 IEEE Vehicle Power and Propulsion Conference (VPPC)* (pp. 1-6). IEEE.
- [24] Pothina, H., & Nagaraja, K. V. (2022) Artificial neural network and math behind it. In *Smart Trends in Computing and Communications: Proceedings of SmartCom 2022*, 205-221. Singapore: Springer Nature Singapore. https://doi.org/10.1007/978-981-16-9967-2_21.
- [25] Ye, J. C., & Ye, J. C. (2022) Artificial Neural Networks and Backpropagation. *Geometry of Deep Learning: A Signal Processing Perspective*, 91-112. https://doi.org/10.1007/978-981-16-6046-7_6.
- [26] Joshi, A. V. (2022). *Perceptron and neural networks*. In *Machine learning and artificial intelligence*, 57-72. Cham: Springer International Publishing. https://doi.org/10.1007/978-3-031-12282-8_6.